nature neuroscience

Article

https://doi.org/10.1038/s41593-026-02221-3

Personalized brain decoding of spontaneous pain in individuals with chronic pain

Received: 25 April 2025

Accepted: 23 January 2026

Published online: 26 February 2026

Check for updates

Jae-Joong Lee[1], Seongwoo Jo[2,6], Sungkun Cho[2] & Choong-Wan Woo[1,3,4,5]

Spontaneous pain is a hallmark of chronic pain disorders, but its assessment remains limited by the lack of objective biomarkers. Here we used precision functional magnetic resonance imaging data, collected over more than half a year from two individuals with chronic pain, to develop personalized brain-decoding models of spontaneous pain. The personalized decoding models accurately tracked fluctuations in spontaneous pain intensity across sessions, runs and minutes (Participant 1: prediction–outcome correlation, $r = 0.40–0.61$; Participant 2: $r = 0.51–0.65$) and effectively discriminated between median-dichotomized high- versus low-pain states (Participant 1: area under the curve = 0.71–0.87; Participant 2: area under the curve = 0.76–0.93). Model performance improved with increased training data, with conventional data quantities failing to achieve significant predictive accuracy. Furthermore, each model relied on individually unique brain features and did not generalize across participants. This study indicates that functional magnetic resonance imaging can assess spontaneous pain, highlighting the need for precise, patient-specific approaches.

Chronic pain is one of the most prevalent healthcare problems and a leading cause of disability[1]. It is characterized by the presence of spontaneous pain, which occurs without an overt noxious stimulus and fluctuates across multiple timescales[2,3]. The current clinical assessment of chronic pain largely relies on self-reported intensity ratings, a measure that is neither fully reliable[4] nor informative about the underlying neurophysiological mechanisms[5]. Pain biomarkers based on brain features could supplement the self-reported measures by providing additional information about pain, offering a pluralistic approach to pain assessment. These biomarkers could also improve our understanding of the neural mechanisms underlying pain and provide a basis for more effective diagnosis and treatment[5].

To date, no brain-based biomarker has demonstrated clinical potential as a surrogate for subjective pain reports. Although a few neuroimaging studies identified brain patterns that track self-reported intensity ratings of stimulus-evoked pain in healthy participants[6–8], their generalizability to stimulus-free spontaneous pain in clinical population remains unclear[9,10]. Furthermore, clinically useful surrogate endpoints should ideally capture the temporal fluctuations of pain within individuals[3,11], a need not addressed by cross-sectional studies predicting pain severity measured at a single time point[8,12,13].

Personalized brain decoding may hold promise for addressing this unmet need[14–16]. This approach involves intensive longitudinal sampling of individuals to develop precise, person-specific brain markers, providing a unique opportunity to directly track intra-individual variations in spontaneous pain[3,17,18]. Importantly, personalized brain decoding leverages densely sampled data of individuals while accounting for interindividual heterogeneity in brain representations, potentially enhancing predictive power[16,18]. This approach has shown promising results in domains such as limb movement[19], speech[20] and depression[21]. However, progress in developing personalized biomarkers for spontaneous pain remains limited.

All existing models have primarily targeted to differentiate between simplified binary states of spontaneous pain (that is, high versus low) and have not been successful in predicting continuous self-reported pain ratings[22], limiting their clinical application, where

[1]Center for Neuroscience Imaging Research, Institute for Basic Science, Suwon, South Korea. [2]Department of Psychology, Chungnam National University, Daejeon, South Korea. [3]Department of Biomedical Engineering, Sungkyunkwan University, Suwon, South Korea. [4]Department of Intelligent Precision Healthcare Convergence, Sungkyunkwan University, Suwon, South Korea. [5]Department of Brain Science and Engineering, Sungkyunkwan University, Suwon, South Korea. [6]Deceased: Seongwoo Jo. e-mail: waniwoo@skku.edu

https://doi.org/10.1038/s41593-026-02221-3

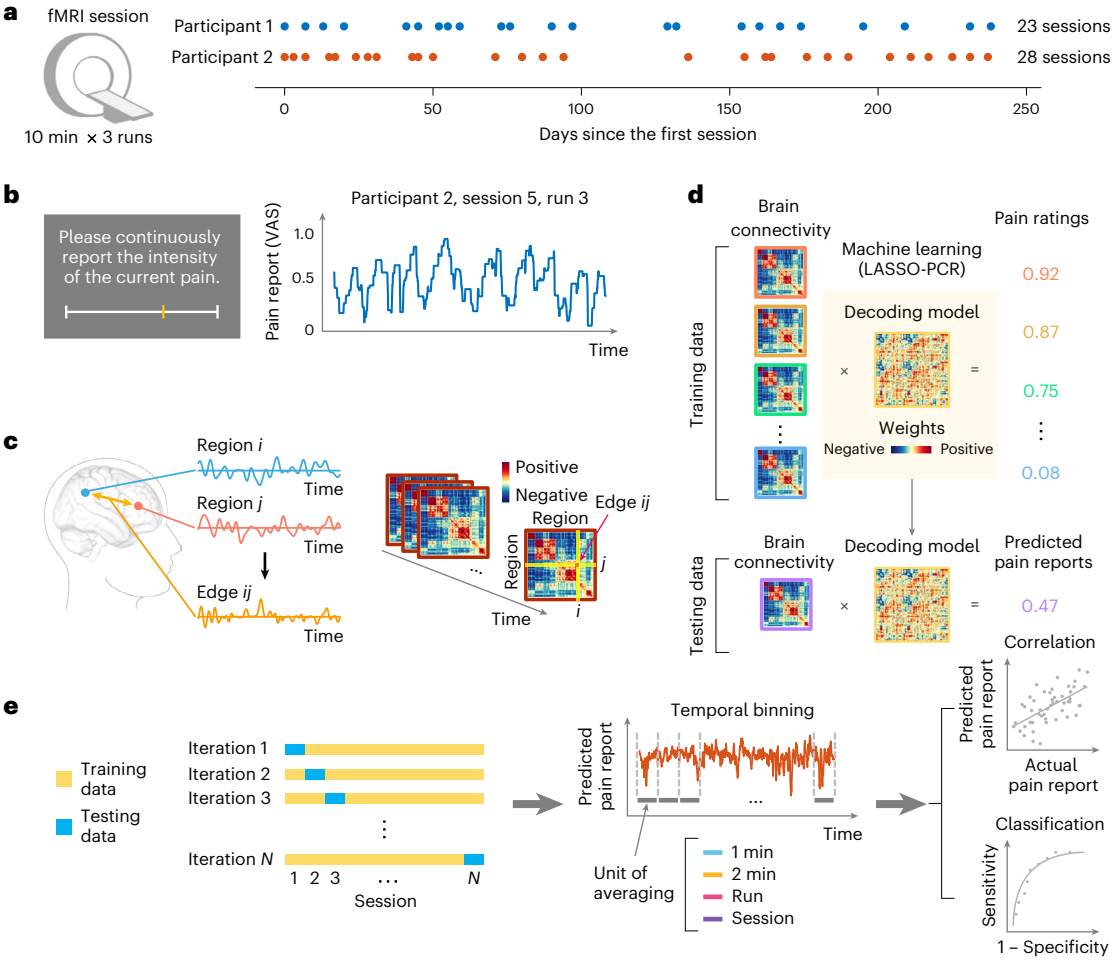

Fig. 1 | Study overview. a, Participants underwent longitudinal, multiple sessions of fMRI scans. Each session consisted of three 10-minute runs. **b**, Participants provided continuous self-reports of spontaneous pain intensity ratings in the scanner. Left: rating instruction and scale. Right: example trajectory of pain reports. **c**, Temporal changes in brain functional connectivity patterns were estimated as edge timeseries, representing the moment-by-moment cofluctuation of fMRI signals between each pair of brain regions. **d**, A machine learning model was trained to predict spontaneous pain reports based on corresponding brain connectivity patterns. The resulting model was tested on a separate dataset not used for training. **e**, Prediction results for each session were obtained from a model trained on all other sessions (that is, cross-validation), which was repeated for all sessions. The continuous timeseries of predicted pain reports was averaged into temporal bins of 1 min, 2 min, one run and one session. Prediction performance was then assessed using Pearson correlation between actual and predicted pain reports or classification accuracy between median-dichotomized high versus low pain. VAS, visual analog scale; neg, negative; pos, positive; LASSO-PCR, least absolute shrinkage and selection operator-regularized principal components regression.

sensitivity to gradual changes in pain is crucial[5,11,23]. Also, previous personalized decoding models have relied on intracranial neural recordings from a restricted number of brain regions[19–22], which may be suboptimal for decoding pain, as pain engages distributed brain networks[6,24,25]. Functional magnetic resonance imaging (fMRI), in contrast, provides a whole-brain measurement with reasonable spatiotemporal resolution and has shown promise in identifying distributed brain patterns associated with self-reported spontaneous pain[8,12,13]. Moreover, fMRI is non-invasive, making it accessible to a broader population of patients with chronic pain. Thus, fMRI offers an advantage over intracranial recordings that require surgical implantation.

Here we investigated whether personalized brain-decoding models based on fMRI could predict fluctuations in spontaneous pain intensity. To this end, we conducted an intensive longitudinal study over more than half a year in individuals with chronic pain, repeatedly measuring self-reported pain alongside whole-brain activity. By leveraging these densely sampled data, we aimed to develop precise, person-specific models capable of tracking moment-by-moment changes in spontaneous pain.

Results

Brain decoding of spontaneous pain intensity

We examined a series of patients ($n = 3$, with two included in the final analyses) with fibromyalgia, a prevalent chronic pain condition characterized by widespread, spontaneous pain[26]. To achieve extensive sampling of brain activity within individuals, participants underwent longitudinal fMRI scanning across multiple sessions on separate days (Fig. 1a). Two of the three enrolled participants completed more than the requisite 15 sessions (Participant 1: 23 sessions; Participant 2: 28 sessions) and are the focus of this study (see Supplementary Fig. 1 for Participant 3's results). Each session consisted of three 10-minute fMRI runs, during which participants provided continuous self-reports of their spontaneous pain (Fig. 1b; see Supplementary Fig. 2 for continuous pain ratings of all runs and sessions). Before the second run, a personalized maneuver was performed to induce naturalistic yet tolerable fluctuations in pain (Participant 1: muscle tightening; Participant 2: straight leg raising; Supplementary Methods).

We estimated concurrent, moment-by-moment changes in brain functional connectivity (that is, edge timeseries[27]) from the fMRI data (Fig. 1c). Note that we employed individual-specific brain

https://doi.org/10.1038/s41593-026-02221-3

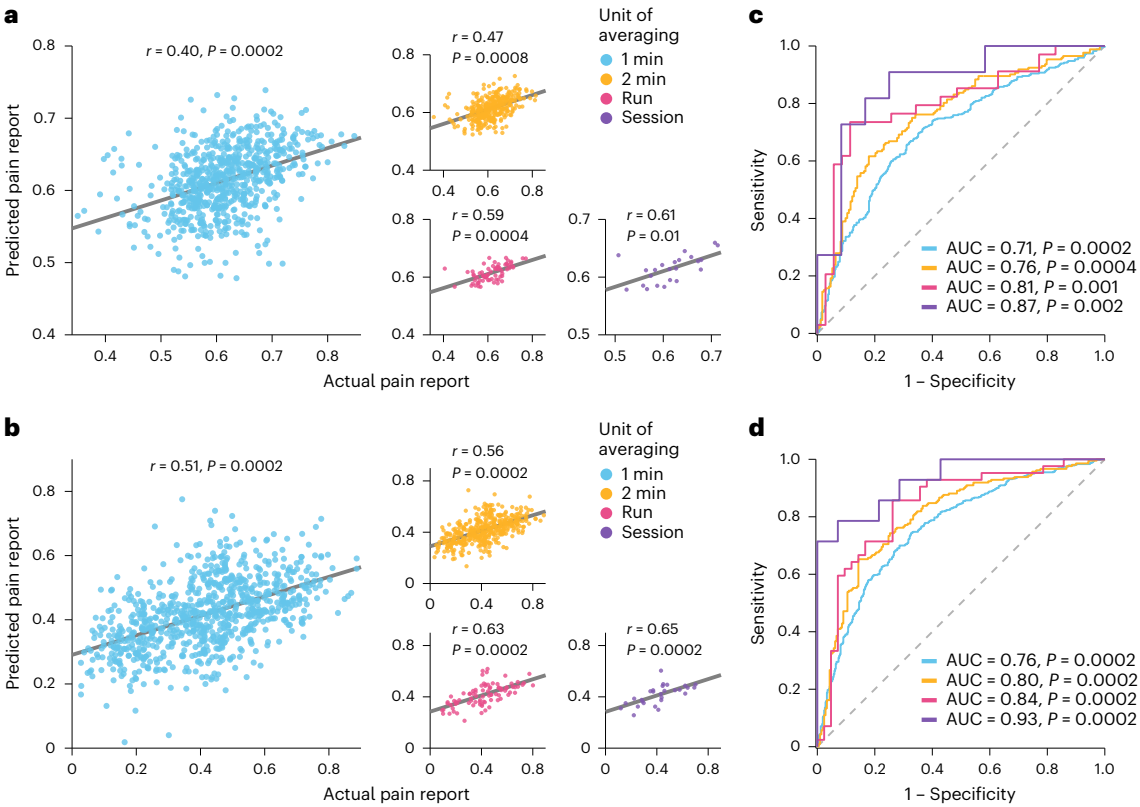

Fig. 2 | Prediction performance. a,**b**, Actual versus predicted pain reports for Participant 1 (**a**) and Participant 2 (**b**). Colors represent the unit of averaging (that is, length of temporal bins). Pearson correlations between actual and predicted pain reports are shown in the plots (Participant 1: 95% CI 0.23–0.55, 0.27–0.65, 0.29–0.82 and 0.17–0.89 for timescales of 1 min, 2 min, run and session, respectively; Participant 2: 95% CI 0.37–0.63, 0.40–0.70, 0.45–0.79 and 0.46–0.82 for the same timescales). **c**,**d**, Receiver operating characteristic (ROC) curves for classifying median-dichotomized high- versus low-pain states for Participant 1 (**c**) and Participant 2 (**d**). Colors represent the unit of averaging. AUC values are shown in the plots (Participant 1: 95% CI 0.62–0.79, 0.65–0.86, 0.63–0.94 and 0.69–1.00 for timescales of 1 min, 2 min, run and session, respectively; Participant 2: 95% CI 0.68–0.84, 0.71–0.88, 0.70–0.94 and 0.82–1.00 for the same timescales). Statistical significance was determined using two-tailed bootstrap tests.

parcellations to derive connectivity features, excluding parcels potentially affected by task-related visual processing to minimize confounds (see Supplementary Fig. 3 for excluded parcels, Supplementary Fig. 4 for decoding results without exclusion and Supplementary Fig. 5 for decoding results using only the excluded vision-related parcels). Using these connectivity patterns, we trained person-specific machine learning models to predict the participants' pain ratings (Fig. 1d). We generated model predictions using cross-validation to separate training and test data and evaluated prediction performance across multiple timescales by varying the unit of temporal averaging (Fig. 1e; see Supplementary Fig. 6 for time-averaged pain ratings of all runs and sessions).

The personalized decoding models accurately tracked moment-by-moment changes in spontaneous pain ratings (Fig. 2a,b). For a timescale of 1 min, the Pearson correlation coefficient between actual and predicted pain ratings was 0.40 (95% CI, 0.23–0.55, $P < 0.001$) for Participant 1 and 0.51 (95% CI, 0.37–0.63, $P < 0.001$) for Participant 2. Prediction performance improved monotonically with longer timescales for both Participant 1 ($r = 0.47, 0.59, 0.61$ for timescales of 2 min, run and session, respectively) and Participant 2 ($r = 0.56, 0.63, 0.65$ for the same timescales, respectively), which may reflect an increased signal-to-noise ratio due to greater temporal averaging[28].

Although the personalized decoding models were not specifically trained for classification, the models could effectively discriminate between median-dichotomized high- versus low-pain states using predicted pain ratings (Fig. 2c,d). For a timescale of 1 min, the area under the receiver operating characteristic curve (AUC) was 0.71 (95% CI, 0.62–0.79, $P < 0.001$) for Participant 1 and 0.76 (95% CI, 0.68–0.84, $P < 0.001$) for Participant 2. Classification performance also improved monotonically with longer timescales for both Participant 1 (AUC = 0.76, 0.81, 0.87 for timescales of 2 min, run and session, respectively) and Participant 2 (AUC = 0.80, 0.84, 0.93 for the same timescales).

In addition, the personalized pain decoding models showed significant prediction performance when evaluated using only the first run, which was not affected by the pain-exacerbating maneuver (Supplementary Fig. 7). The models were also able to predict session-to-session variations in spontaneous pain ratings based on the resting-state fMRI data, which did not involve any rating procedure and was not used in model training (Supplementary Fig. 8). Furthermore, the models did not show significant performance when using only the vision-related parcels (Supplementary Fig. 9).

The personalized pain decoding models were sensitive not only to changes across multiple sessions but also to within-run and within-session variations (Supplementary Fig. 10). Furthermore, model predictions were not significantly associated with head motion (Supplementary Fig. 11). Decoding based on a population-level brain parcellation also yielded significant prediction performance (Supplementary Fig. 12). However, an a priori decoding model of sustained pain—the Tonic Pain Signature[8], which was developed to capture functional connectivity patterns generalizable at the group level—did not show significant prediction performance in either participant (Supplementary Fig. 13). Together, these findings support the validity of personalized fMRI models in capturing ongoing, spontaneous pain.

https://doi.org/10.1038/s41593-026-02221-3

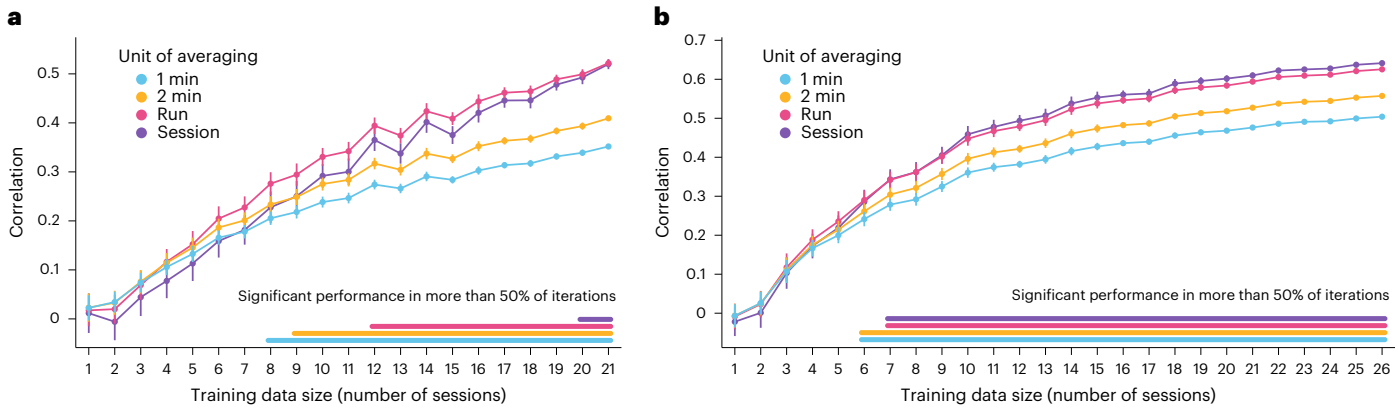

Fig. 3 | Effect of training data size on decoding performance. a,**b**, Pearson correlations between actual and predicted pain reports from personalized decoding models trained on varying amounts of data for Participant 1 (**a**) and Participant 2 (**b**). Each dot represents the mean correlation coefficient across 100 iterations of random subsampling. Error bars indicate the 95% CI. Colors represent the unit of averaging. The number of sessions that yielded significant decoding performance in more than half of the 100 iterations is marked as colored horizontal lines above the *x* axis of the plot.

Effect of training data size on decoding performance

To evaluate how the amount of training data influences decoding accuracy, we systematically varied the number of fMRI sessions used to train the personalized models. For each training size, we randomly selected sessions from the full training set during each fold of cross-validation, repeating this procedure 100 times to ensure stability and robustness. We then calculated the Pearson correlation coefficients between actual and predicted pain ratings for each iteration and examined how these correlations changed with increasing training data.

Decoding performance improved as the training data size increased (Fig. 3). We found a significant linear relationship between the number of training sessions and the mean correlation coefficients across all 100 iterations of random subsampling for both Participant 1 ($\hat{\beta}$ = 57.48, 50.18, 37.53, 36.70 and t_{19} = 17.15, 17.46, 20.07, 27.47, for timescales of 1 min, 2 min, run and session, respectively; subscript denotes degrees of freedom; all *P* values < 0.001) and Participant 2 ($\hat{\beta}$ = 47.51, 42.56, 37.22, 34.89 and t_{24} = 12.06, 12.19, 11.92, 11.79, for the same timescales; subscript denotes degrees of freedom; all *P* values < 0.001).

The minimum number of sessions required to achieve significant decoding performance in more than half of the 100 iterations was 8, 9, 12 and 20 for timescales of 1 min, 2 min, run and session in Participant 1 and 6, 6, 7 and 7 for the same timescales in Participant 2. These numbers exceed the typical number of fMRI sessions (for example, four or five) in previous longitudinal studies on chronic pain[17,29], highlighting the importance of extensive sampling.

To further examine the role of data variability beyond quantity alone, we additionally trained models using the first 12 sessions, rather than randomly subsampling the same number of sessions from the full datasets (Supplementary Fig. 14). We chose 12 sessions because this matched the total number of sessions available for Participant 3, thereby allowing a direct comparison. Interestingly, these models did not show significant prediction performance for either Participant 1 or Participant 2, despite using the same amount of training data. This finding suggests that model generalization depends not only on dataset size but also on the diversity and representativeness of the training data. Random subsampling from a larger dataset likely helps capture a broader range of variability in the data[30], which appears to be critical for successful decoding and generalizability and may also explain the poor decoding performance observed in Participant 3 (Supplementary Fig. 1).

Person-specific model weights and brain features

To investigate the individual specificity of our personalized brain-decoding models, we first identified key brain features that contributed to spontaneous pain prediction within each participant using a permutation-based feature importance analysis. This method assesses each brain region's contribution by quantifying the drop in model performance when all connections to that region are randomly permuted.

The results showed that the personalized decoding models relied on individually distinct brain features for prediction (Fig. 4). For Participant 1, brain regions with high feature importance included the left temporal pole and right posterior hippocampus, which are known to be involved in semantic and episodic memory[31,32] and may play a role in learning and memory aspects of pain[33,34]. In contrast, the important brain regions for Participant 2 included the left premotor and primary somatomotor cortices, which have been primarily associated with the sensory-discriminative aspect of pain in previous literature[35,36]. To aid interpretation further, we mapped the important regions for each participant onto personalized canonical functional brain networks (Supplementary Fig. 15; for details on identifying personalized brain networks, see Supplementary Methods). These regions were distributed across multiple networks, which differed between participants, suggesting that spontaneous pain may be decoded by individually distinct brain systems that span multiple functional domains. We also present univariate general linear model analysis results using pain intensity as the independent variable in Supplementary Fig. 16.

To further evaluate individual specificity beyond visual inspection of feature maps, we performed cross-testing of the personalized brain-decoding models (Fig. 5). Specifically, we used the model trained on Participant 2 to predict pain ratings for Participant 1 and vice versa. Each participant's model failed to predict the other participant's pain, resulting in non-significant prediction–outcome correlations (r = −0.05 to 0.04 and r = −0.27 to −0.07, across all the timescales) and classification performances (AUC = 0.49–0.56 and AUC = 0.48–0.52, across all the timescales), suggesting the models' individual specificity. Cross-testing of models derived from a population-level brain parcellation also yielded non-significant results (Supplementary Fig. 17), suggesting that this individual specificity was not simply due to the use of personalized brain parcellations.

Discussion

In this study, we developed personalized decoding models of spontaneous pain based on densely sampled fMRI data. These models predicted changes in pain ratings and discriminated between high- versus low-pain states across timescales ranging from minutes to days. Prediction accuracy was associated with training data size, with conventional data quantities failing to achieve significant predictions. The models

https://doi.org/10.1038/s41593-026-02221-3

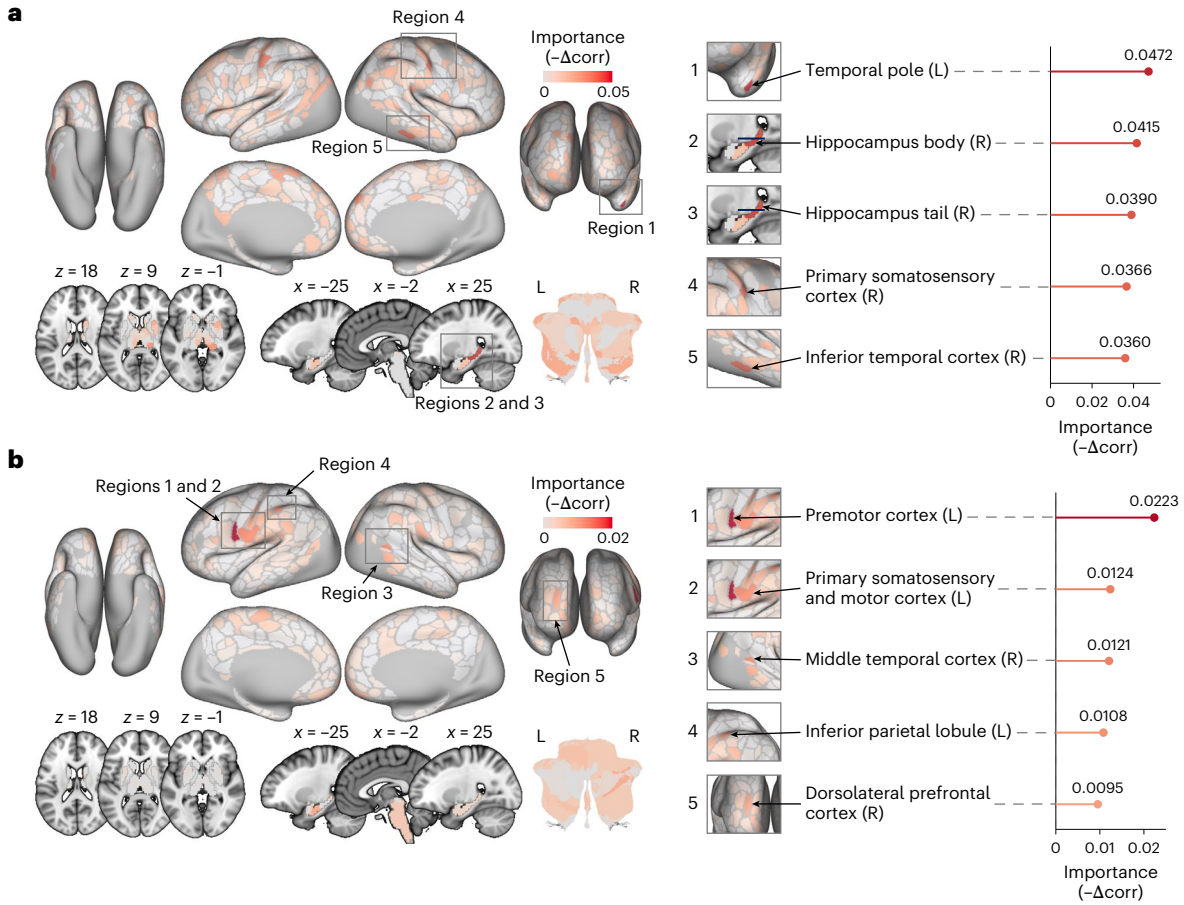

Fig. 4 | Feature importance maps. a,**b**, Permutation-based feature importance maps of personalized pain decoding models for Participant 1 (**a**) and Participant 2 (**b**). Mean decrease of prediction–outcome correlation (−Δcorr) after permutation was used as a measure of feature importance. To optimize visualization, brain regions with negative feature importance were set to zero. The top five brain regions with the highest feature importance are highlighted.

relied on individual-specific brain features and could not predict the pain ratings of other participants, highlighting their specificity at the individual level.

Despite the distributed nature of pain processing[6,24,25], previous personalized decoding of spontaneous pain has been limited to recording from a few selected brain regions[22]. This study employed fMRI to address this limitation by identifying whole-brain interaction patterns associated with spontaneous pain. The significant decoding of spontaneous pain ratings across multiple timescales, which was not successful with local intracranial recordings[22], highlights the importance of modeling global brain activity in chronic pain[25]. These findings further suggest the potential of neuroimaging to provide an objective assessment for disease progression and treatment response in chronic pain, leading to more informed clinical decision-making and guiding the development of targeted therapeutics[5,11].

We demonstrated that extensive sampling of fMRI data is essential for accurate prediction. However, not all individuals with chronic pain can undergo multiple fMRI sessions due to mobility limitations, discomfort from prolonged scanning and the high cost of MRI. Therefore, it is important to consider the feasibility and clinical utility of this approach for clinical translation. In addition, more time-efficient methods for acquiring high-quality data, such as multi-echo fMRI[37], could help expand accessibility to a broader patient population.

The individual specificity of prediction models emphasizes the heterogeneity of chronic pain[17] and the importance of a personalized approach[14–16]. For example, we observed that memory-related regions, including the hippocampus and temporal pole, were important for Participant 1, whereas sensorimotor-related regions, including premotor and primary somatomotor cortices, were important for Participant 2. One possibility is that the difference in pain duration (Participant 1: 7 years versus Participant 2: 10 months) may lead to distinct influences of pain-related memory[38] and sensorimotor functions[39] on pain, which warrants further investigation.

It is important to note that the decoding models in our study context may rely on neural signals that are non-specific to pain, because our study did not include a specificity condition during model training and testing. As a result, the models can draw on any reliable corollary information distributed across the brain, potentially including signals related to memory, salience, self-monitoring and the introspective evaluation of pain. In this sense, our decoding maps may be more individual-specific and more spatially distributed than pain-encoding maps or than decoding maps explicitly trained for pain specificity. Accordingly, the high degree of individual specificity observed in our decoding models may reflect not only heterogeneity in pain-related neural processing itself but also person-specific factors that shape the available decoding signals. These factors may include differences in pain chronicity, past experience and memory, as well as variability in task-related pain introspection, ongoing medication use and broader disease-related neural plasticity.

Despite this individual specificity, it remains possible that generalizable brain representations exist within certain subtypes of patients[40]. Given the small number of participants in the present study, however, we were unable to identify potential subtypes or systematically examine the sources of this variability. Addressing these questions

https://doi.org/10.1038/s41593-026-02221-3

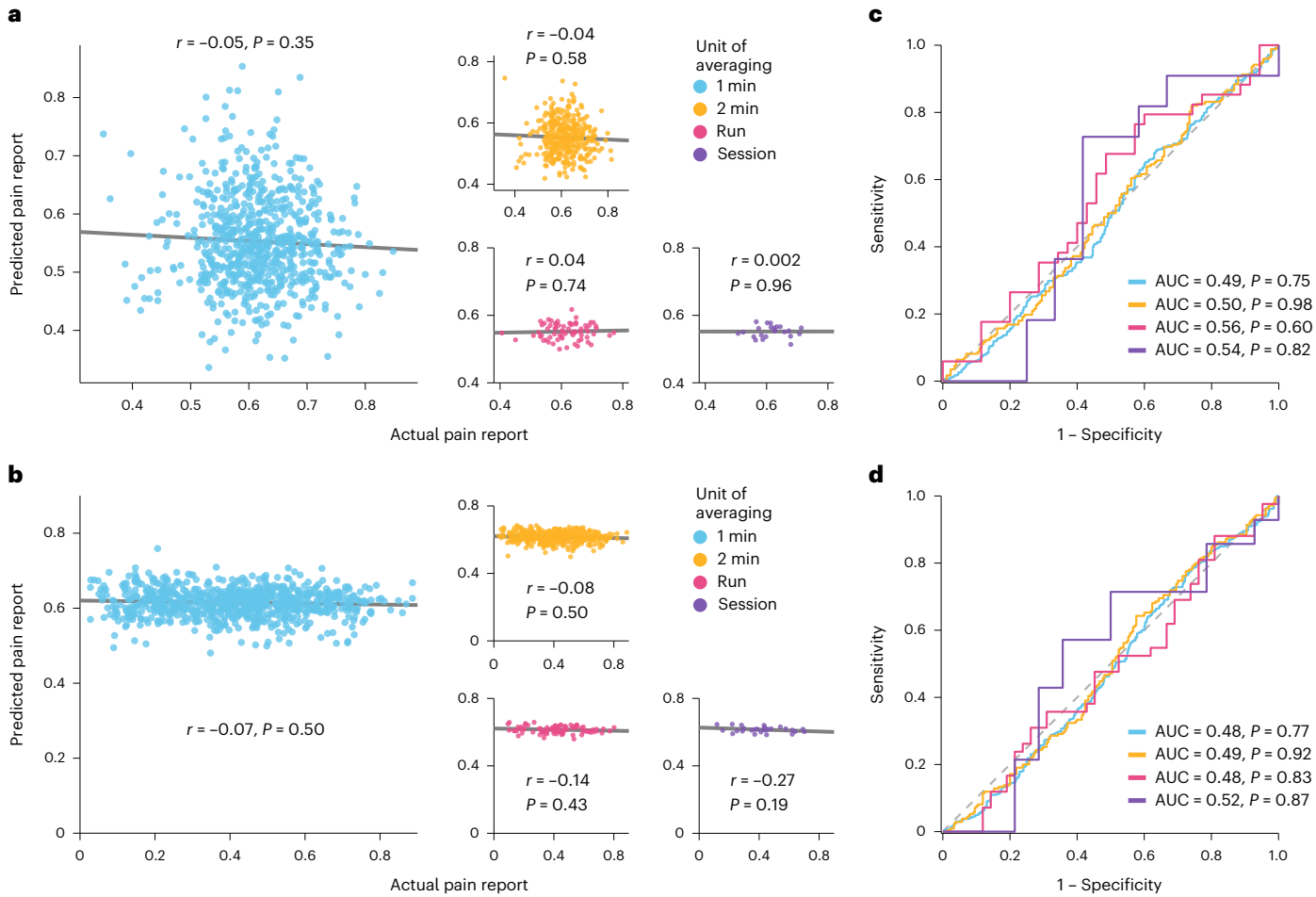

Fig. 5 | Cross-testing of personalized decoding models. We predicted the pain reports of Participant 1 using the decoding model of Participant 2 and the pain reports of Participant 2 using the decoding model of Participant 1. **a**,**b**, Actual versus predicted pain reports for Participant 1 (**a**) and Participant 2 (**b**). Colors represent the unit of averaging. Pearson correlations between actual and predicted pain report are shown in the plots (Participant 1: 95% CI −0.16 to 0.06, −0.20 to 0.11, −0.24 to 0.31 and −0.36 to 0.39 for timescales of 1 min, 2 min, run and session, respectively; Participant 2: 95% CI −0.24 to 0.12, −0.29 to 0.14, −0.42 to 0.21 and −0.59 to 0.14 for the same timescales). **c**,**d**, ROC curves for classifying median-dichotomized high- versus low-pain states for Participant 1 (**c**) and Participant 2 (**d**). Colors represent the unit of averaging. AUC values are shown in the plots (Participant 1: 95% CI 0.42–0.56, 0.40–0.60, 0.35–0.75 and 0.29–0.80 for timescales of 1 min, 2 min, run and session, respectively; Participant 2: 95% CI 0.38–0.58, 0.36–0.62, 0.30–0.66 and 0.29–0.75 for the same timescales). Statistical significance was determined using two-tailed bootstrap tests.

represents a promising direction for future research and will require larger samples and experimental designs to enable causal testing.

Overall, our study presents a new opportunity to identify personalized biomarkers for spontaneous pain with clinical validity for single patients, which could potentially advance the diagnosis and treatment of chronic pain.

Online content

Any methods, additional references, Nature Portfolio reporting summaries, source data, extended data, supplementary information, acknowledgements, peer review information; details of author contributions and competing interests; and statements of data and code availability are available at https://doi.org/10.1038/s41593-026-02221-3.

References

1. Dahlhamer, J. et al. Prevalence of chronic pain and high-impact chronic pain among adults - United States, 2016. *MMWR Morb. Mortal. Wkly Rep.* **67**, 1001–1006 (2018).
2. Foss, J. M., Apkarian, A. V. & Chialvo, D. R. Dynamics of pain: fractal dimension of temporal variability of spontaneous pain differentiates between pain States. *J. Neurophysiol.* **95**, 730–736 (2006).
3. Mun, C. J. et al. Investigating intraindividual pain variability: methods, applications, issues, and directions. *Pain* **160**, 2415–2429 (2019).
4. Smith, S. M. et al. Pain intensity rating training: results from an exploratory study of the ACTTION PROTECCT system. *Pain* **157**, 1056–1064 (2016).
5. Davis, K. D. et al. Discovery and validation of biomarkers to aid the development of safe and effective pain therapeutics: challenges and opportunities. *Nat. Rev. Neurol.* **16**, 381–400 (2020).
6. Wager, T. D. et al. An fMRI-based neurologic signature of physical pain. *N. Engl. J. Med.* **368**, 1388–1397 (2013).
7. Woo, C. W. et al. Quantifying cerebral contributions to pain beyond nociception. *Nat. Commun.* **8**, 14211 (2017).
8. Lee, J. J. et al. A neuroimaging biomarker for sustained experimental and clinical pain. *Nat. Med.* **27**, 174–182 (2021).
9. Baliki, M. N. et al. Chronic pain and the emotional brain: specific brain activity associated with spontaneous fluctuations of intensity of chronic back pain. *J. Neurosci.* **26**, 12165–12173 (2006).
10. Jaillard, A. & Ropper, A. H. Pain, heat, and emotion with functional MRI. *N. Engl. J. Med.* **368**, 1447–1449 (2013).

11. FDA-NIH Biomarker Working Group. *BEST (Biomarkers, EndpointS, and other Tools) Resource* (FDA, 2016).
12. Cheng, J. C. et al. Multivariate machine learning distinguishes cross-network dynamic functional connectivity patterns in state and trait neuropathic pain. *Pain* **159**, 1764–1776 (2018).
13. Lee, J. et al. Machine learning-based prediction of clinical pain using multimodal neuroimaging and autonomic metrics. *Pain* **160**, 550–560 (2019).
14. Gordon, E. M. et al. Precision functional mapping of individual human brains. *Neuron* **95**, 791–807 e797 (2017).
15. Porter, A. et al. Masked features of task states found in individual brain networks. *Cereb. Cortex* **33**, 2879–2900 (2023).
16. Kraus, B. et al. Insights from personalized models of brain and behavior for identifying biomarkers in psychiatry. *Neurosci. Biobehav Rev.* **152**, 105259 (2023).
17. Mayr, A. et al. Patients with chronic pain exhibit individually unique cortical signatures of pain encoding. *Hum. Brain Mapp.* **43**, 1676–1693 (2022).
18. Reddan, M. C. Recommendations for the development of socioeconomically-situated and clinically-relevant neuroimaging models of pain. *Front. Neurol.* **12**, 700833 (2021).
19. Vansteensel, M. J. et al. Fully implanted brain-computer interface in a locked-in patient with ALS. *N. Engl. J. Med.* **375**, 2060–2066 (2016).
20. Moses, D. A. et al. Neuroprosthesis for decoding speech in a paralyzed person with anarthria. *N. Engl. J. Med.* **385**, 217–227 (2021).
21. Alagapan, S. et al. Cingulate dynamics track depression recovery with deep brain stimulation. *Nature* **622**, 130–138 (2023).
22. Shirvalkar, P. et al. First-in-human prediction of chronic pain state using intracranial neural biomarkers. *Nat. Neurosci.* **26**, 1090–1099 (2023).
23. Altman, D. G. & Royston, P. The cost of dichotomising continuous variables. *Br. Med. J.* **332**, 1080 (2006).
24. Coghill, R. C. The distributed nociceptive system: a framework for understanding pain. *Trends Neurosci.* **43**, 780–794 (2020).
25. Farmer, M. A., Baliki, M. N. & Apkarian, A. V. A dynamic network perspective of chronic pain. *Neurosci. Lett.* **520**, 197–203 (2012).
26. Clauw, D. J. Fibromyalgia: a clinical review. *JAMA* **311**, 1547–1555 (2014).
27. Zamani Esfahlani, F. et al. High-amplitude cofluctuations in cortical activity drive functional connectivity. *Proc. Natl Acad. Sci. USA* **117**, 28393–28401 (2020).
28. Lee, D. H., Lee, S. & Woo, C. W. Decoding pain: uncovering the factors that affect the performance of neuroimaging-based pain models. *Pain* **166**, 360–375 (2025).
29. Hashmi, J. A. et al. Shape shifting pain: chronification of back pain shifts brain representation from nociceptive to emotional circuits. *Brain* **136**, 2751–2768 (2013).
30. Ooi, L. Q. R. et al. Longer scans boost prediction and cut costs in brain-wide association studies. *Nature* **644**, 731–740 (2025).
31. Patterson, K., Nestor, P. J. & Rogers, T. T. Where do you know what you know? The representation of semantic knowledge in the human brain. *Nat. Rev. Neurosci.* **8**, 976–987 (2007).
32. Setton, R., Mwilambwe-Tshilobo, L., Sheldon, S., Turner, G. R. & Spreng, R. N. Hippocampus and temporal pole functional connectivity is associated with age and individual differences in autobiographical memory. *Proc. Natl Acad. Sci. USA* **119**, e2203039119 (2022).
33. Moulton, E. A. et al. Painful heat reveals hyperexcitability of the temporal pole in interictal and ictal migraine States. *Cereb. Cortex* **21**, 435–448 (2011).
34. Branco, P. et al. Hippocampal functional connectivity after whiplash injury is linked to the development of chronic pain. *Nat. Ment. Health* **2**, 1362–1370 (2024).
35. Coghill, R. C., Sang, C. N., Maisog, J. M. & Iadarola, M. J. Pain intensity processing within the human brain: a bilateral, distributed mechanism. *J. Neurophysiol.* **82**, 1934–1943 (1999).
36. Frot, M., Magnin, M., Mauguiere, F. & Garcia-Larrea, L. Cortical representation of pain in primary sensory-motor areas (S1/M1)—a study using intracortical recordings in humans. *Hum. Brain Mapp.* **34**, 2655–2668 (2013).
37. Lynch, C. J. et al. Rapid precision functional mapping of individuals using multi-echo fMRI. *Cell Rep.* **33**, 108540 (2020).
38. Apkarian, A. V. Pain perception in relation to emotional learning. *Curr. Opin. Neurobiol.* **18**, 464–468 (2008).
39. Kim, J. et al. Somatotopically specific primary somatosensory connectivity to salience and default mode networks encodes clinical pain. *Pain* **160**, 1594–1605 (2019).
40. Drysdale, A. T. et al. Resting-state connectivity biomarkers define neurophysiological subtypes of depression. *Nat. Med.* **23**, 28–38 (2017).

Methods

Participants

We studied patients with fibromyalgia, a common type of chronic pain disorder primarily characterized by chronic widespread pain. Participants were eligible for enrollment if they had a confirmed diagnosis of fibromyalgia and had been experiencing pain for more than six months, with an average intensity greater than 4/10 on the visual analog scale. We excluded participants with chronic secondary pain (for example, autoimmune disease, tumor, fracture or infection), a history of substance use disorder, MRI contraindications, left-handedness or previous experience with psychological interventions. Three participants who met the inclusion and exclusion criteria were recruited from the general public of South Korea through online advertisement and telephone interviews.

Participant 1 was a 44-year-old woman who had experienced pain since childhood. Her first episode of pain occurred without preceding physical injuries, and she was diagnosed with fibromyalgia seven years before enrollment. Participant 2 was a 37-year-old woman who developed pain after a traffic accident one year and four months before enrollment, although physical and radiological examinations at the time of the accident showed no signs of physical injury. She had a confirmed diagnosis of fibromyalgia ten months before enrollment. Participant 3 was a 37-year-old woman who reported that her pain began a week after giving birth and was diagnosed with fibromyalgia seven years before enrollment.

The overall pain intensity scores at the time of enrollment were 5 out of 10, 7 out of 10 and 7 out of 10 on the visual analog scale for Participants 1, 2 and 3, respectively. All participants were taking medications to manage their symptoms (Participant 1: pregabalin, tramadol, milnacipran, celecoxib; Participant 2: pregabalin, celecoxib, trazodone, sertraline, alprazolam; Participant 3: antidepressants and anxiolytics (declined to specify the exact medications)). All participants provided written informed consent. The institutional review board of Sungkyunkwan University approved the study (approval number 2021-08-013).

Study design

We conducted longitudinal, multisession fMRI scans (for details on data acquisition and preprocessing, see Supplementary Methods). The total number of planned fMRI sessions was 30, with a minimum requirement of 15 sessions for inclusion in the study. Participants were encouraged to complete as many sessions as possible. Two of the three enrolled participants completed more than 15 fMRI sessions (Participant 1: 23 sessions; Participant 2: 28 sessions; Participant 3: 12 sessions); therefore, we present analysis results from Participants 1 and 2 here (Fig. 1a; see Supplementary Fig. 1 for Participant 3's results).

Each fMRI session consisted of a resting condition and three distinct experimental tasks (for details, see Supplementary Methods). In this study, we used the spontaneous pain rating task data to train and test personalized pain decoding models. The spontaneous pain rating task consisted of three 10-minute runs. During this task, participants continuously reported their moment-by-moment spontaneous pain intensity using a trackball mouse (Fig. 1b). To induce fluctuations in spontaneous pain in a naturalistic and tolerable manner, participants performed an individualized physical maneuver while lying on the bed before the second run (for details, see Supplementary Methods). Participants were instructed to continue their medications to ensure safe participation in the experiment.

Training and evaluation of personalized pain decoding models

We developed personalized decoding models for spontaneous pain as follows. First, we removed the initial 66 volumes (30 s) of fMRI images, which could be affected by initial rating motion, and shifted the timing of these images by 13 volumes (6 s) to account for the hemodynamic delay. Then, we averaged the voxel-wise fMRI data within the individual-specific brain parcels (for details on deriving individual-specific parcellation, see Supplementary Methods). We excluded parcels in the occipital areas and those assigned to the visual network from further analyses to mitigate potential confounds from visual processing of the rating bar (Supplementary Fig. 3).

We then estimated the moment-by-moment whole-brain cofluctuations by computing the framewise product of z-standardized fMRI signals between each pair of brain parcels. This method, termed 'edge timeseries'[27], provides a measure of instantaneous inter-regional connectivity (Fig. 1c). The edge timeseries and the corresponding spontaneous pain ratings were binned into deciles by sorting the pain ratings within each run into ten levels of pain intensity. We then averaged the edge timeseries and pain ratings within each bin to use them as the dependent and independent variables in model training. We trained decoding models that predicted the binned average pain ratings based on the binned average edge timeseries data using the least absolute shrinkage and selection operator-regularized principal components regression algorithm (Fig. 1d; Supplementary Methods).

We tested the models on edge timeseries data that were not used for model training (Fig. 1e). The separation of training and test data was based on leave-one-session-out cross-validation, which could provide less biased estimates of prediction performance while maximizing the training sample size. The predicted continuous pain ratings were then averaged into temporal bins. We used time-based binning instead of intensity-based binning, as it does not require rating information for binning, making it better suited for unbiased tests. The averaging units were 10 bins per run (1 min), 5 bins per run (2 mins), a run (10 mins) and a session (30 mins), each representing decoding results at different timescales. We assessed the prediction performance by calculating the Pearson correlation between actual and predicted pain reports. For the other metrics, including coefficients of determination (R^2) and mean absolute error, please see Supplementary Table 1. We also evaluated classification performance for median-dichotomized high- versus low-pain states by computing the AUC.

Training size dependence

To examine the impact of the training data size on prediction performance, we trained the decoding models while varying the number of training sessions. For each iteration of leave-one-session-out cross-validation, we randomly selected a given number of sessions from the training set instead of using all available sessions. We repeated this random subsampling procedure 100 times per cross-validation iteration and for each training set size. We kept the regularization parameter for each iteration the same as in the original model. We then calculated correlation coefficients between actual and predicted pain reports for each iteration of random subsampling. We assessed the linear relationship between the number of training sessions and mean correlation coefficients across all 100 iterations using linear regression. We also determined the minimum number of training sessions that yielded a statistically significant correlation coefficient ($P < 0.05$) in more than half of the 100 iterations.

Feature importance

To identify the key brain features for decoding spontaneous pain within individuals, we measured permutation-based feature importance from the personalized decoding models. In this approach, we randomly permuted a set of brain features from the final model and measured the resulting changes in prediction performance. A large decline in performance indicates that the permuted features have an important contribution to the prediction. We assessed the permutation feature importance of each brain region by removing all its connections (that is, edge timeseries) to the region from the decoding model and calculating the decrease in prediction performance at the 10-bins-per-run version (that is, one minute-level) test data using leave-one-session-out cross-validation. We repeated the permutation

procedure 10,000 times and used the average performance decrease as the feature importance score.

Statistical analysis

We set 15 sessions as the minimum requirement for the main analysis. This minimum number of sessions ensures 80% power to detect a correlation of $r = 0.66$, which represents the median of the individual-level correlation coefficients between prefrontal gamma oscillations and spontaneous pain intensity[41]. The 15 sessions provide 7.5 h of fMRI data, which corresponded to the minimum training data required to reach a performance plateau for personalized decoding models, as reported in a previous study[42].

We computed 95% confidence intervals (CIs) and statistical significance of correlation coefficients and AUCs using bootstrap tests with 10,000 iterations. To account for dependence in longitudinal data, we obtained bootstrap samples sequentially at each level of the data hierarchy (for example, session, run and time-bin)[43]. For run-level prediction, we obtained bootstrap samples first from sessions and then from runs within the selected sessions. For time-bin-level prediction, we also obtained bootstrap samples sequentially from sessions, from runs for the selected sessions and then from time-bins within the selected runs.

Reporting summary

Further information on research design is available in the Nature Portfolio Reporting Summary linked to this article.

Data availability

Raw MRI data are publicly available at https://openneuro.org/datasets/ds006815. All the data to generate the figures are available via figshare at https://doi.org/10.6084/m9.figshare.31064431 (ref. 44). Source data are provided with this paper.

Code availability

Code for the main analyses is available via GitHub at https://github.com/cocoanlab/DEIPP (ref. 45).

References

41. May, E. S. et al. Prefrontal gamma oscillations reflect ongoing pain intensity in chronic back pain patients. *Hum. Brain Mapp.* **40**, 293–305 (2019).
42. Tang, J., LeBel, A., Jain, S. & Huth, A. G. Semantic reconstruction of continuous language from non-invasive brain recordings. *Nat. Neurosci.* **26**, 858–866 (2023).
43. Saravanan, V., Berman, G. J. & Sober, S. J. Application of the hierarchical bootstrap to multi-level data in neuroscience. *Neuron. Behav. Data Anal. Theory* **3**, 1–25 (2020).
44. Lee, J.-J. & Woo, C. W. DEIPP. *figshare* https://doi.org/10.6084/m9.figshare.31064431 (2026).
45. Lee, J.-J. et al. Repository for "Personalized Brain Decoding of Spontaneous Pain in Individuals With Chronic Pain". *GitHub* https://github.com/cocoanlab/DEIPP (2025).

Acknowledgements

We thank all patients for their participation in this study. We thank J. Lee and S.-G. Kim for help with participant recruitment. We thank E.-J. Jeong, J. Han and Y. Park for help with conducting experiments. This work was supported by Institute for Basic Science (grant no. IBS-R015-D2 to C.-W.W.).

Author contributions

J.-J.L. and C.-W.W. conceived and designed the experiment. S.J. and S.C. contributed to the experimental design, participant management and psychotherapy. J.-J.L. conducted the data analysis. J.-J.L. and C.-W.W. interpreted the results. J.-J.L. wrote the manuscript. C.-W.W. provided supervision and edited the manuscript. All authors reviewed and approved the final manuscript, except for S.J., who passed away in November 2023.

Competing interests

The authors declare no competing interests.

Additional information

Supplementary information The online version contains supplementary material available at https://doi.org/10.1038/s41593-026-02221-3.

Correspondence and requests for materials should be addressed to Choong-Wan Woo.

Peer review information *Nature Neuroscience* thanks Benjamin Becker, Markus Ploner and the other, anonymous, reviewer(s) for their contribution to the peer review of this work.

nature portfolio

Corresponding author(s): Choong-Wan Woo

Last updated by author(s): Jan 13, 2026

Reporting Summary

Nature Portfolio wishes to improve the reproducibility of the work that we publish. This form provides structure for consistency and transparency in reporting. For further information on Nature Portfolio policies, see our Editorial Policies and the Editorial Policy Checklist.

Statistics

For all statistical analyses, confirm that the following items are present in the figure legend, table legend, main text, or Methods section.

n/a	Confirmed	
☐	☒	The exact sample size (*n*) for each experimental group/condition, given as a discrete number and unit of measurement
☐	☒	A statement on whether measurements were taken from distinct samples or whether the same sample was measured repeatedly
☐	☒	The statistical test(s) used AND whether they are one- or two-sided *Only common tests should be described solely by name; describe more complex techniques in the Methods section.*
☐	☒	A description of all covariates tested
☐	☒	A description of any assumptions or corrections, such as tests of normality and adjustment for multiple comparisons
☐	☒	A full description of the statistical parameters including central tendency (e.g. means) or other basic estimates (e.g. regression coefficient) AND variation (e.g. standard deviation) or associated estimates of uncertainty (e.g. confidence intervals)
☐	☒	For null hypothesis testing, the test statistic (e.g. *F*, *t*, *r*) with confidence intervals, effect sizes, degrees of freedom and *P* value noted *Give P values as exact values whenever suitable.*
☒	☐	For Bayesian analysis, information on the choice of priors and Markov chain Monte Carlo settings
☐	☒	For hierarchical and complex designs, identification of the appropriate level for tests and full reporting of outcomes
☐	☒	Estimates of effect sizes (e.g. Cohen's *d*, Pearson's *r*), indicating how they were calculated

Our web collection on statistics for biologists contains articles on many of the points above.

Software and code

Policy information about availability of computer code

Data collection	We collected data using Psychtoolbox (version 3.0, http://psychtoolbox.org/) running on Matlab (version 2017a, Mathworks).
Data analysis	Code for preprocessing and main analyses is available on Github (https://github.com/cocoanlab/DEIPP).

For manuscripts utilizing custom algorithms or software that are central to the research but not yet described in published literature, software must be made available to editors and reviewers. We strongly encourage code deposition in a community repository (e.g. GitHub). See the Nature Portfolio guidelines for submitting code & software for further information.

Data

Policy information about availability of data

All manuscripts must include a data availability statement. This statement should provide the following information, where applicable:

- Accession codes, unique identifiers, or web links for publicly available datasets
- A description of any restrictions on data availability
- For clinical datasets or third party data, please ensure that the statement adheres to our policy

Raw MRI data are publicly available at https://openneuro.org/datasets/ds006815. All the data to generate the figures are available at https://doi.org/10.6084/m9.figshare.31064431.

Research involving human participants, their data, or biological material

Policy information about studies with human participants or human data. See also policy information about sex, gender (identity/presentation), and sexual orientation and race, ethnicity and racism.

Reporting on sex and gender	This study included three female participants. The sex and gender of participants were collected by self-report. We did not perform sex- or gender-based analysis.
Reporting on race, ethnicity, or other socially relevant groupings	N/A
Population characteristics	The participants were aged 44, 37, and 37 years and had been diagnosed with fibromyalgia.
Recruitment	The participants were recruited from the general public of South Korea through online advertisement and telephone interviews. While this recruitment approach may introduce self-selection bias toward motivated individuals who can tolerate and complete repeated MRI sessions, the main analyses focus on within-participant prediction evaluated on held-out sessions.
Ethics oversight	The institutional review board of the Sunkyunkwan University approved the study (approval number 2021-08-013). All participants provided written informed consent for the participation.

Note that full information on the approval of the study protocol must also be provided in the manuscript.

Field-specific reporting

Please select the one below that is the best fit for your research. If you are not sure, read the appropriate sections before making your selection.

☒ Life sciences ☐ Behavioural & social sciences ☐ Ecological, evolutionary & environmental sciences

For a reference copy of the document with all sections, see nature.com/documents/nr-reporting-summary-flat.pdf

Life sciences study design

All studies must disclose on these points even when the disclosure is negative.

Sample size	This study employed an intensive longitudinal design, with a minimum requirement of 15 sessions per participant for inclusion in the main analysis. This threshold was set to ensure 80% statistical power to detect a correlation of r = 0.66, which represents the median of the individual-level correlation coefficients between prefrontal gamma oscillations and spontaneous pain intensity (May et al., 2019). The 15 sessions provide 7.5 hours of fMRI data, which corresponded to the minimum training data required to reach a performance plateau for personalized decoding models, as reported in a previous study (Tang et al., 2023). Three participants completed 23, 28, and 13 sessions, respectively. Therefore, the two participants who completed more than the requisite 15 sessions are the focus of this study.
Data exclusions	The participant who completed fewer than 15 sessions (Participant 3) was excluded from the primary analyses.
Replication	We used leave-one-session-out cross-validation to evaluate the decoding performance of the personalized models on each participant's unseen data. To assess the individual specificity of the models, we also tested each model on data from a different participant. No additional independent cohorts were collected.
Randomization	No randomization was needed for this study because there was no experimental group allocation.
Blinding	No blinding was needed for this study because there was no experimental group allocation.

Reporting for specific materials, systems and methods

We require information from authors about some types of materials, experimental systems and methods used in many studies. Here, indicate whether each material, system or method listed is relevant to your study. If you are not sure if a list item applies to your research, read the appropriate section before selecting a response.

Materials & experimental systems

n/a	Involved in the study
☒	☐ Antibodies
☒	☐ Eukaryotic cell lines
☒	☐ Palaeontology and archaeology
☒	☐ Animals and other organisms
☒	☐ Clinical data
☒	☐ Dual use research of concern
☒	☐ Plants

Methods

n/a	Involved in the study
☒	☐ ChIP-seq
☒	☐ Flow cytometry
☐	☒ MRI-based neuroimaging

Plants

Seed stocks

Report on the source of all seed stocks or other plant material used. If applicable, state the seed stock centre and catalogue number. If plant specimens were collected from the field, describe the collection location, date and sampling procedures.

Novel plant genotypes

Describe the methods by which all novel plant genotypes were produced. This includes those generated by transgenic approaches, gene editing, chemical/radiation-based mutagenesis and hybridization. For transgenic lines, describe the transformation method, the number of independent lines analyzed and the generation upon which experiments were performed. For gene-edited lines, describe the editor used, the endogenous sequence targeted for editing, the targeting guide RNA sequence (if applicable) and how the editor was applied.

Authentication

Describe any authentication procedures for each seed stock used or novel genotype generated. Describe any experiments used to assess the effect of a mutation and, where applicable, how potential secondary effects (e.g. second site T-DNA insertions, mosiacism, off-target gene editing) were examined.

Magnetic resonance imaging

Experimental design

Design type

Resting state, block design task

Design specifications

Each fMRI session consisted of a resting condition and three distinct experimental tasks (spontaneous pain rating, speaking, listening). This study used the (1) resting state data for deriving individual-specific brain parcels and networks and generalizability testing, and (2) spontaneous pain rating task data for training and testing personalized pain decoding models.
(1) Resting state: One run, each for 10 minutes
(2) Spontaneous pain rating task: Three runs, each for 10 minutes

Behavioral performance measures

For (2) spontaneous pain rating task, participants continuously reported their moment-by-moment spontaneous pain intensity using a trackball mouse.

Acquisition

Imaging type(s)

Functional, structural

Field strength

3 Tesla

Sequence & imaging parameters

Imaging was performed using a 3T Siemens Prisma scanner at Sungkyunkwan University. For each session, whole-brain fMRI images were acquired using a gradient-echo EPI sequence with TR = 460 ms, TE = 26 ms, flip angle = 90 degrees, multiband acceleration factor = 8, field of view = 216 mm, 80 × 80 × 56 matrix, 2.7 × 2.7 × 2.7 mm voxels. We also acquired the two spin-echo EPI scans, one with the same phase encoding direction as the fMRI images and the other with the reversed phase encoding direction. For the session 1, 11, and 21, T1-weighted structural images were acquired with TR = 2400 ms, TE = 2.34 ms, TI = 1150 ms, flip angle = 8 degrees, 224 × 320 × 320 matrix, 0.7 × 0.7 × 0.7 mm voxels. For the session 2, 12, and 22, T2-weighted structural images were acquired with TR = 3100 ms, TE = 566 ms, 224 × 320 × 320 matrix, 0.7 × 0.7 × 0.7 mm voxels.

Area of acquisition

Whole brain

Diffusion MRI ☐ Used ☒ Not used

Preprocessing

Preprocessing software

FSL 6.0
Freesurfer 7.2
AFNI 23.0
ciftify (https://github.com/edickie/ciftify/)
Code for preprocessing: https://github.com/cocoanlab/DEIPP

Normalization	Combining linear transformation (BOLD -> T1) and non-linear transformation (T1 -> MNI)
Normalization template	MNI152
Noise and artifact removal	We conducted motion censoring, denoising, and temporal filtering using AFNI ('3dTproject'). First, the motion-contaminated volumes with framewise displacement (FD) > 0.2 mm were removed and replaced through linear interpolation over time. To prevent overly aggressive motion censoring due to respiratory artifacts, head motion parameters were low pass-filtered (< 0.1 Hz) prior to FD calculation. Subsequently, denoising and temporal filtering were carried out in a single nuisance regression step. Regressors for denoising include a linear trend, 6 head motion parameters derived from motion correction, 5 principal components of white matter (WM) signals and 5 principal components of cerebrospinal fluid (CSF) signals. For temporal filtering, we applied band-pass filter (0.005 Hz – 0.1 Hz) for the resting condition and high-pass filter (> 0.005 Hz) for the other conditions.
Volume censoring	The motion-contaminated volumes as defined above (FD > 0.2 mm) were excluded from further analyses.

Statistical modeling & inference

Model type and settings	We used the principal component regression with LASSO regularization to predict tonic pain ratings based on whole-brain edge timeseries features.
Effect(s) tested	We calculated Pearson's correlation between actual and predicted pain reports within individuals as a primary indicator of prediction performance. We also evaluated classification performance for median-dichotomized high vs. low pain states by computing the area under the receiver-operating-characteristic curve (AUC).

Specify type of analysis: ☒ Whole brain ☐ ROI-based ☐ Both

Statistic type for inference (See Eklund et al. 2016)	This study used edge timeseries methods for inference.
Correction	We used false discovery rate (FDR) correction method.

Models & analysis

n/a	Involved in the study
☐	☒ Functional and/or effective connectivity
☒	☐ Graph analysis
☐	☒ Multivariate modeling or predictive analysis

Functional and/or effective connectivity	We computed the framewise product of z-standardized fMRI signals between each pair of brain parcels (i.e., edge timeseries) to derive a measure of instantaneous inter-regional functional connectivity.
Multivariate modeling and predictive analysis	We used the principal component regression (PCR) with LASSO regularization to predict pain ratings across time based on whole-brain edge timeseries features. First, we reduced the dimensionality of the edge timeseries features using the principal component analysis (PCA). Then, the principal component scores were used as the predictor variables of LASSO regression to predict pain ratings. The selection of LASSO regularization parameter (λ) and model evaluation was performed using nested cross-validation.